DALTON
FULL PAPER

Reactions of tetrathiotungstate and tetrathiomolybdate with substituted haloalkanes

Jian-Ping Lang,[a,b] Hiroyuki Kawaguchi[a] and Kazuyuki Tatsumi *[a]

[a] *Research Center for Materials Science and Department of Chemistry, Graduate School of Science, Nagoya University, Furo-cho, Chikusa-ku, Nagoya 464-8602, Japan. E-mail: i45100a@nucc.cc.nagoya-u.ac.jp*
[b] *Department of Chemistry and Chemical Engineering, Suzhou University, 1 Shizhi Street, Jiangsu, Suzhou 215006, P. R. China*

Received 23rd July 2001, Accepted 23rd April 2002
First published as an Advance Article on the web 16th May 2002

Reactions of $[PPh_4]_2[WS_4]$ in CH_3CN with excess n-hexylbromide, 1,4-dichlorobutane, 2-(bromomethyl)tetrahydro-2*H*-pyran) (bmthp), and 2-(bromoethyl)-1,3-dioxane (bedo) followed by extraction with THF afforded a series of alkylthiolatotrithiotungstate complexes, $[PPh_4][(RS)WS_3]$ (**1**: R = n-hexyl; **2**: R = $ClCH_2CH_2CH_2CH_2$; **3**: R = mthp; **4**: R = edo), and the analogous reactions of $[PPh_4]_2[MoS_4]$ in CH_3CN–THF with excess bmthp and bedo also generated $[PPh_4][(RS)MoS_3]$ (**5**: R = mthp; **6**: R = edo), albeit in low yields. Treatment of $[PPh_4]_2[WS_4]$ in CH_3CN with excess (*S*)-(+)-3-bromo-2-methyl-1-propanol turned out to give a trinuclear, $[PPh_4]_2[W_3S_8((S)\text{-}(+)\text{-}OCH_2CH(Me)CH_2Br)_2]$ (**7**). Compounds **1**–**7** were characterized spectroscopically and the crystal structures of **2**–**7** were determined by X-ray analysis. All the mononuclear complexes **2**–**6** assume tetrahedral structures, being coordinated by one thiolate sulfur and three terminal sulfido ligands, and no additional coordination was observed by the O-donor portions of mthp or edo. The structure of **7** consists of a linear W_3 spine and two (*S*)-(+)-$OCH_2CH(Me)CH_2Br$ ligands are coordinated at the central W atom.

Introduction

The rich chemistry of tetrathiomolybdate and tetrathiotungstate $[MS_4]^{2-}$ (M = Mo, W) is well documented.[1–9] It is rather surprising that a seemingly simple alkylation reaction of these tetrathiometallates to give $[(RS)MS_3]^-$ did not emerge until the pioneering work by Boorman *et al.* was communicated.[10a] They were successful in isolating $[PPh_4][(Et–S)WS_3]$ from the reaction between $[PPh_4]_2[WS_4]$ and EtBr under carefully controlled conditions. Later, the synthesis of other alkylated complexes, $[PPh_4][(^tBu–S)MoS_3]$ and $[PPh_4][(RS)WS_3]$ (R = ^{i}Pr, ^{i}Bu, ^{t}Bu, benzyl, allyl), were reported by the same group.[10b–d] The analogous trithio(thiolato) complexes of niobium and tantalum, $[NEt_4]_2[(^tBuS)MS_3]$ (M = Nb, Ta) are available, which were obtained directly from the reactions of $NbCl_5$ or $TaCl_5$ with NaS^tBu in the presence of elemental sulfur.[11]

We have been particularly interested in developing the chemistry of mononuclear sulfido complexes of Group 6 transition metals, and use of pentamethylcyclopentadienyl as an auxiliary ligand allowed us to isolate the trisulfido complexes, $[PPh_4][(\eta^5\text{-}C_5Me_5)MS_3]$ (M = Mo, W).[12] The terminal sulfido ligands of these trisulfido complexes were found to react readily with alkynes and haloalkynes, and were also shown to serve as convenient building blocks for various heterometallic cluster syntheses.[13] As an extension of the chemistry of "mononuclear" trisulfido complexes of molybdenum and tungsten, we have investigated alkylation reactions of $[PPh_4]_2[WS_4]$ and $[PPh_4]_2[MoS_4]$ with various substituted haloalkanes. Reported herein are six new complexes of the type $[PPh_4][(RS)MS_3]$ (M = W: **1**, R = n-hexyl; **2**, R = $ClCH_2CH_2CH_2CH_2$; **3**, R = mthp; **4**, R = edo; M = Mo: **5**, R = mthp; **6**, R = edo) obtained therefrom. In the case of the reaction between $[PPh_4]_2[WS_4]$ and (*S*)-(+)-3-bromo-2-methyl-1-propanol, a linear trinuclear cluster $[PPh_4]_2[W_3S_8(OCH_2CH(Me)CH_2Br)_2]$ (**7**) was isolated. The crystal structures of **2**–**7**, determined by single-crystal X-ray analysis, are described, and their electronic properties and solution behavior are discussed based on the IR, UV-vis, and ESI-mass spectra.

Results and discussion

Alkylation reactions of $[PPh_4]_2[WS_4]$ and $[PPh_4]_2[MoS_4]$

We first attempted the reaction of non-substituted alkylbromide with $[PPh_4]_2[WS_4]$. Thus, as a six-fold excess of n-hexylbromide was added to a yellow solution of $[PPh_4]_2[WS_4]$ in CH_3CN, the color of the solution turned red immediately. After stirring the red solution at room temperature for 2 h, the solvent was removed *in vacuo* and the resulting solids were extracted with THF. The THF extract was concentrated to *ca.* 4 mL and layered with diethyl ether, from which $[PPh_4]$-[(n-hexyl-S)WS_3] (**1**) was isolated as red crystals in 73% yield based on $[PPh_4]_2[WS_4]$. We then examined the reactions of $[PPh_4]_2[WS_4]$ with the substituted haloalkanes; 1,4-dichlorobutane, 2-(bromomethyl)tetrahydro-2*H*-pyran (bmthp), and 2-(bromoethyl)-1,3-dioxane (bedo). These reactions proceeded smoothly, and after a workup similar to the one used for the synthesis of **1**, the alkylated products $[PPh_4][(RS)WS_3]$ (**2**, R = $ClCH_2CH_2CH_2CH_2$; **3**, R = mthp; **4**, R = edo) were isolated in 63, 81, and 71% yields, respectively.

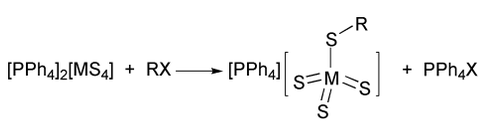

(1)

M = W: **1**, R = n-hexyl
2, R = $CH_2CH_2CH_2CH_2Cl$
3, R = mthp
4, R = edo
M = Mo: **5**, R = mthp
6, R = edo

DOI: 10.1039/b106572f

On the other hand, isolation of the alkylated products of tetrathiomolybdate is more problematic. Reactions of $[PPh_4]_2[MoS_4]$ with a six-fold excess of bmthp or bedo in THF–CH_3CN (3 : 2 v/v) gave a dark red–brown homogeneous solution. After removing all solvents at 0 °C and extracting with THF, the extract was concentrated to 4 mL at 0 °C and filtered again. The filtrate was layered with Et_2O and allowed to stand at −5 °C. From these procedures **5** and **6** were isolated in low yield, 15 and 12%, respectively. As will be described later in this paper, formation of the desired alkylated complexes of tetrathiomolybdate in the reaction systems was confirmed by ESI mass spectroscopy. However, during the removal of THF–CH_3CN solvents, concentration of the THF extracts and subsequent crystallization in THF–Et_2O, a large amount of an insoluble black powder always precipitated. Thus the low yields for **5** and **6** are due to degradation occurring in the process of isolation. The X-ray fluorescence microanalysis of the insoluble black powder suggests that it could be MoS_2 and/or MoS_3.

Complexes **1**–**6** are stable in the solid state when kept under argon, and they gradually decompose upon exposure to air. They dissolve readily in CH_3CN, THF, and $CHCl_3$, but are insoluble in CH_3OH and Et_2O. The tungsten complexes **1**–**4** are relatively stable in dilute CH_3CN while at higher concentrations they tend to slowly degrade. A similar trend was also noticed for $[PPh_4][(EtS)WS_3]$.[11] The CH_3CN solutions of molybdenum complexes, **5** and **6**, are much less stable. Intriguingly, the molybdenum complexes appear to be more stable in THF, which is why the preparations of **5** and **6** were carried out in a THF–CH_3CN mixed solvent.

The alkylation reactions of tetrathiometallates occur at one S atom only and the remaining three terminal sulfides do not react with excess haloalkanes. This phenomenon is relevant to the reactions of $[(\eta^5\text{-}C_5Me_5)MS_3]^-$ with various haloalkanes.[13c,d] We also noted that the rates of the alkylation reactions of $[PPh_4]_2[WS_4]$ vary substantially depending on haloalkanes. For example, the reaction of $[PPh_4]_2[WS_4]$ with n-hexylbromide is completed in 2 h, while it takes 4 days for completion of the reaction with 1,4-dichlorobutane. The longer reaction time for 1,4-dichlorobutane may be due to the stronger C–Cl bond. A steric factor of the R group may come into play in determining the reaction rate as well, as the reaction with bmthp takes 2 days, while that with bedo is completed in 8 h. Interestingly, when these reaction systems are kept stirring for a prolonged period, degradation of the alkylated product begins to occur, generating the trinuclear cluster $[PPh_4]_2[W_3S_9]$.[14] For instance, when a CH_3CN solution of $[PPh_4]_2[WS_4]$ and excess n-hexylbromide was stirred for 10 h, the alkylated complex **1** could not be obtained, and dark red crystals of $[PPh_4]_2[W_3S_9]$ were isolated in *ca.* 70% yield. After removal of this product, the filtrate was analyzed by GC/MS and we detected formation of $(CH_3CH_2CH_2CH_2CH_2CH_2)_2S$ and $(CH_3CH_2CH_2CH_2CH_2CH_2)_2S_2$.

A kinetic study by Boorman *et al.* suggests that decomposition of $[PPh_4][(Et–S)WS_3]$ is a second-order reaction.[10b,15] Assuming that this is also the case for decomposition of **1**–**4**, we propose a decomposition pathway as shown in Scheme 1. In this mechanism, association of two molecules of $[PPh_4][(RS)WS_3]$ must be the rate determining step. This assumption is not labored, for the tungsten center of $[(RS)WS_3]^-$ is coordinatively less saturated compared with $[WS_4]^{2-}$. Dissociation of two RS groups from the W^{VI}–W^{VI} dinuclear structure would generate $(S)_2W^V(\mu\text{-}S)_2W^V(S)_2$ and R_2S_2. Then addition of $[(RS)WS_3]^-$ to $[(S)_2W^V(\mu\text{-}S)_2W^V(S)_2]^{2-}$ and subsequent loss of RS^- gives rise to $[W_3S_9]^{2-}$ which consists of a W^{VI}–W^{IV}–W^{VI} trinuclear framework. And RX in the reaction system may react with RS^-, leading to formation of RSR.

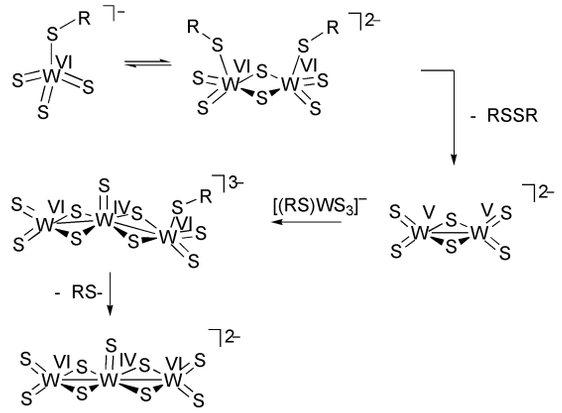

Scheme 1

Reaction of $[PPh_4]_2[WS_4]$ with (*S*)-(+)-3-bromo-2-methyl-1-propanol

In an attempt to synthesize an alkylated complex $[PPh_4][(R^*S)WS_3]$ having a chiral R* group, we examined the reaction of $[PPh_4]_2[WS_4]$ in CH_3CN with excess (*S*)-(+)-3-bromo-2-methyl-1-propanol. However, alkylation at sulfur did not occur. Instead, trinuclear compounds, $[PPh_4]_2[W_3S_8((S)\text{-}(+)\text{-}OCH_2CH(Me)CH_2Br)_2]$ (**7**) and $[PPh_4]_2[W_3S_9]$ were isolated as red leaf-shape crystals (32% yield) and dark red microcrystalline solids (47% yield), respectively. Apparently the alcoholic OH group of (*S*)-(+)-3-bromo-2-methyl-1-propanol is the reaction site, and the C–Br bond remains intact. Only H_2S was detected by GC/MS analysis of the volatile substances trapped from the CH_3CN solution at liquid nitrogen temperature. The air-stable crystals of **7** dissolve readily in DMF, DMSO, and are slightly soluble in CH_3CN.

$$[PPh_4]_2[WS_4] + (S)\text{-}(+)\text{-}HOCH_2CH(Me)CH_2Br \longrightarrow [PPh_4]_2[\mathbf{7}] + [PPh_4]_2[W_3S_9] \quad (2)$$

7, $R^* = (+)\text{-}CH_2CH(Me)CH_2Br$

It is known that $(NH_4)_2[WS_4]$ and $[PPh_4]_2[WS_4]$ are aggregated to polynuclear tungstensulfides in acidic media. For example, $[W_3S_9]^{2-}$ was formed upon acidification of a CH_2Cl_2 solution of $[PPh_4]_2[WS_4]$ with 3.5 M acetic acid.[14] When 0.1 M HCl was added to a dilute aqueous solution of $[WS_4]^{2-}$, $[W_3OS_8(H_2O)]^{2-}$ was generated,[16] while acidification of a dilute aqueous solution of $(NH_4)_2[WS_4]$ with dilute H_2SO_4 resulted in $[W_3S_8]^{2-}$.[17] The important steps in the formation of polynuclear tungstensulfides are the protonation at a sulfur atom of $[WS_4]^{2-}$ and the subsequent intramolecular redox reactions.[1,11,18] These three trinuclear complexes, $[W_3S_9]^{2-}$, $[W_3OS_8(H_2O)]^{2-}$, and $[W_3S_8]^{2-}$, have a common $[W_3S_8]$ core similar to that of **7**, as is discussed later in this paper. Therefore formation of **7** and $[PPh_4]_2[W_3S_9]$ may be ascribable to the acidic nature of the OH group of (*S*)-(+)-3-bromo-2-methyl-1-propanol. In order to verify the above consideration, the following experiments were carried out.

A CH_3CN solution of $[PPh_4]_2[WS_4]$ was treated with excess propanol or iso-propanol for 4 days to check that no reaction took place. However, when excess 3-bromopropanol was added to $[PPh_4]_2[WS_4]$ in the same solvent, an immediate color change, from yellow to dark-red, was observed and we isolated dark red microcrystals of $[PPh_4]_2[W_3S_9]$ in 75% yield. Again H_2S is a single volatile substance detected by GC/MS from the CH_3CN solution. Formation of $(HOCH_2CH(Me)CH_2)_2S$ and/or $(HOCH_2CH(Me)CH_2)_2S_2$ was not discernible. The bromo-substituted alcohol, 3-bromopropanol, seems to be more acidic than unsubstituted propanol and iso-propanol. After removal of $[PPh_4]_2[W_3S_9]$ from the reaction system, the dark red plates of $[PPh_4]_2[W_4S_{12}]$ were formed in <1% yield upon standing the remaining CH_3CN solution, which was characterized by X-ray analysis. The tetranuclear cluster, $[PPh_4]_2[W_4S_{12}]$, is known to be

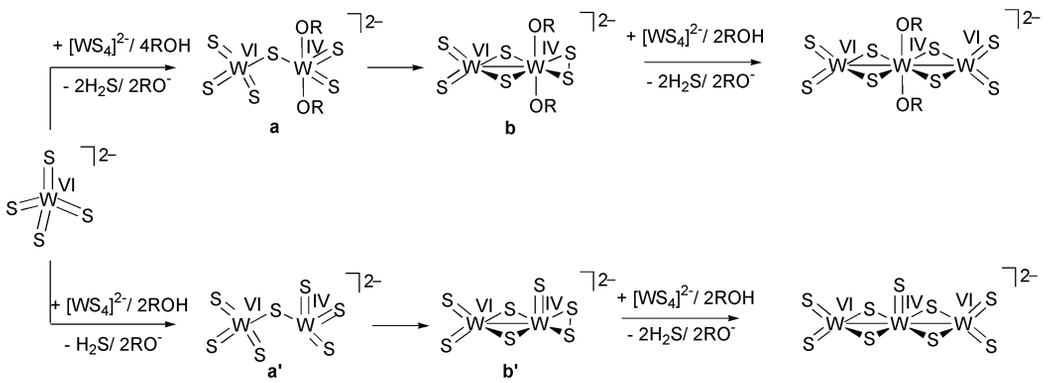

Scheme 2

formed from a CH_2Cl_2 solution of $[PPh_4]_2[WS_4]$ by acidification with acetic acid.[19]

$$[WS_4]^{2-} + HOCH_2CH_2CH_2Br \not\longrightarrow [W_3S_8(OCH_2CH_2CH_2Br)_2]_2- \quad (3)$$

$$\longrightarrow [W_3S_9]^{2-} + [W_4S_{12}]_2-$$

We also found that the preformed trinuclear sulfido cluster $[PPh_4]_2[W_3S_9]$ did not react with either excess (*S*)-(+)-3-bromo-2-methyl-1-propanol or propanol. These alcohols do not react with alkylated tetrathiotungstates, *e.g.*, $[PPh_4][(mthp\text{-}S)WS_3]$ (**3**), too. Thus the conversion of $[W_3S_9]^{2-}$ to $[W_3S_8(OR)_2]^{2-}$ in the presence of excess ROH is unlikely to occur. Also ruled out is the possibility that the alkylated complex $[PPh_4][((S)\text{-}(+)\text{-}HOCH_2CH(Me)CH_2S)WS_3]$ is first formed and then transformed to **7** in the presence of excess (*S*)-(+)-3-bromo-2-methyl-1-propanol. With these results in mind, we suggest the pathways to **7** and $[PPh_4]_2[W_3S_9]$ as shown in Scheme 2. In the proposed mechanism, one equivalent of $[WS_4]^{2-}$ is first acidified by ROH (R = (*S*)-(+)-3-bromo-2-methyl-1-propyl) and the following reactions with another equivalent of $[WS_4]^{2-}$ generate dinuclear complexes **a** and **a′**. In these processes, H_2S is created while the oxidation states of the W centers remain VI. Subsequently, **a** or **a′** undergoes intramolecular redox reaction to form complexes **b** and **b′**. Finally, **b** and **b′** react with $[WS_4]^{2-}$ leading to $[W_3S_8(OR)_2]^{2-}$ and $[W_3S_9]^{2-}$, respectively.

Crystal structures of $[PPh_4][(RS)MS_3]$ (M = W: 2, R = $ClCH_2CH_2CH_2$; 3, R = mthp; 4, R = edo; M = Mo: 5, R = mthp; 6, R = edo)

Of a series of newly synthesized alkylated complexes, $[PPh_4][(RS)MS_3]$, **2**, **4**, and **6** crystallize in the common monoclinic space group $P2_1/c$, while **3** and **5** crystallize in the triclinic space group $P\bar{1}$. Crystals of **3** and **4** are isomorphous to those of **5** and **6**, respectively. The structures of the complex anions of **2**–**6** are very similar to that of $[PPh_4][(EtS)WS_3]$.[10a] We show only the crystal structures of **4** and **5** in Fig. 1 and 2, and the selected bond lengths and angles of **2**–**6** are compared in Table 1. In each structure, the Mo(VI) or W(VI) atom is coordinated by three sulfides and a thiolate sulfur in an approximately tetrahedral geometry. The bond lengths between the metal centers and thiolate sulfurs are 0.17–0.25 Å longer than the average M=S double bonds. The ideal tetrahedral structure of $[MS_4]^{2-}$ is not distorted by much upon alkylation. In the structures of **3**–**6**, both tetrahydro-2*H*-pyran and 1,3-dioxane rings adopt a chair conformation, and the MS_3SCH_2– and $MS_3SCH_2CH_2$– moieties occupy the equatorial positions of the six-membered rings. We anticipated that the oxygen atoms of tetrahydro-2*H*-pyran and 1,3-dioxane rings might coordinate to the electron-deficient W(VI) and Mo(VI) centers, and that the alkylated complexes would be stabilized by formation of five- or six-membered metallacycles. However, this is not the case for **3**–**6** according to the X-ray study.

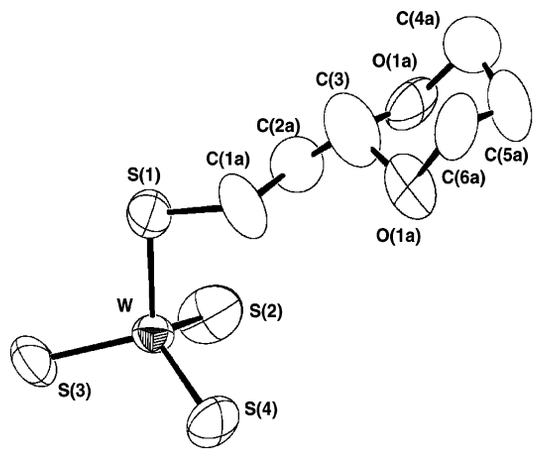

Fig. 1 Structure of $[(edo\text{-}S)WS_3]^-$ (**4**), where only the disordered edo atoms which were refined with a site occupancy factor of 0.50 are shown. The thermal ellipsoids represent 50% probability surfaces. Hydrogen atoms are omitted for clarity.

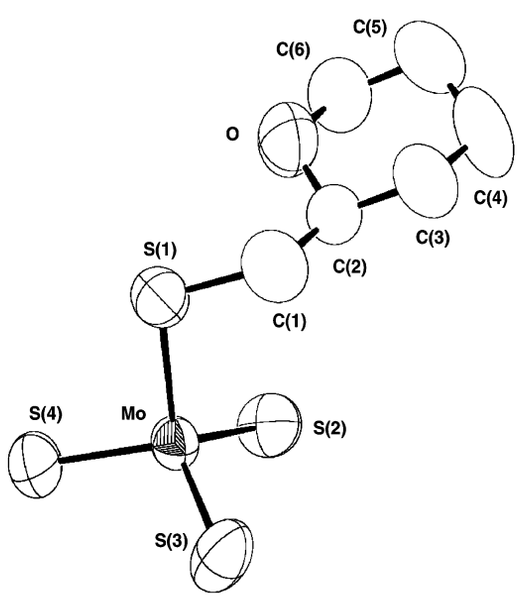

Fig. 2 Structure of $[(mthp\text{-}S)MoS_3]^-$ (**5**). The thermal ellipsoids represent 50% probability surfaces. Hydrogen atoms are omitted for clarity.

Crystal structure of $[PPh_4]_2[W_3S_8((S)\text{-}(+)\text{-}OCH_2CH(Me)CH_2Br)_2]$ (7)

Complex **7** crystallizes in the triclinic space group $P\bar{1}$, and the asymmetric unit contains one crystallographically-independent $[W_3S_8((S)\text{-}(+)\text{-}OCH_2CH(Me)CH_2Br)_2]^{2-}$ dianion and two $[PPh_4]^+$ cations. Fig. 3 shows the crystal structure of

Table 1 Comparison of the selected bond lengths (Å) and angles (°) for **2**–**6**

	2	**3**	**4**	**5**	**6**
W(Mo)–S(1)	2.313(5)	2.327(2)	2.308(2)	2.338(1)	2.318(3)
W(Mo)–S(2)	2.128(4)	2.150(2)	2.146(3)	2.132(2)	2.134(3)
W(Mo)–S(3)	2.133(4)	2.143(2)	2.147(2)	2.131(2)	2.149(2)
W(Mo)–S(4)	2.148(4)	2.137(2)	2.137(2)	2.143(2)	2.126(3)
S(1)–W(Mo)–S(2)	109.0(2)	109.94(9)	108.9(1)	110.52(7)	109.2(1)
S(1)–W(Mo)–S(3)	105.0(2)	110.3(1)	101.89(9)	99.96(6)	101.58(10)
S(1)–W(Mo)–S(4)	108.7(2)	100.26(8)	109.5(1)	110.07(6)	109.3(1)
S(2)–W(Mo)–S(4)	112.4(2)	114.1(1)	110.4(1)	109.92(6)	113.6(1)
W(Mo)–S(1)–C(1)	107.0(7)	106.8(3)	105.7[a]	106.2(2)	106.2[a]

[a] Average value of two disordered structures.

Table 2 Selected bond lengths (Å) and angles (°) of **7**

W(1)–W(2)	3.0006(8)	W(2)–W(3)	2.9973(9)
W(1)–S(1)	2.169(4)	W(1)–S(2)	2.147(3)
W(1)–S(3)	2.270(3)	W(1)–S(4)	2.253(3)
W(2)–S(3)	2.484(3)	W(2)–S(4)	2.429(4)
W(2)–S(5)	2.472(3)	W(2)–S(6)	2.427(3)
W(3)–S(5)	2.257 (3)	W(3)–S(6)	2.244(4)
W(3)–S(7)	2.172(4)	W(3)–S(8)	2.142(4)
W(2)–O(1)	1.886(9)	W(2)–O(2)	1.828(8)
W(1)–W(2)–W(3)	179.20(3)	W(1)–W(2)–O(1)	88.8(3)
W(1)–W(2)–O(2)	91.8(3)	W(3)–W(2)–O(1)	90.7(3)
W(3)–W(2)–O(2)	88.7(3)	W(1)–S(3)–W(2)	78.12(9)
W(1)–S(4)–W(2)	79.61(10)	W(2)–S(5)–W(3)	78.50(10)
W(2)–S(6)–W(3)	79.73(10)	W(2)–O(1)–C(1)	141.1(8)
W(2)–O(2)–C(5)	142.3(7)		

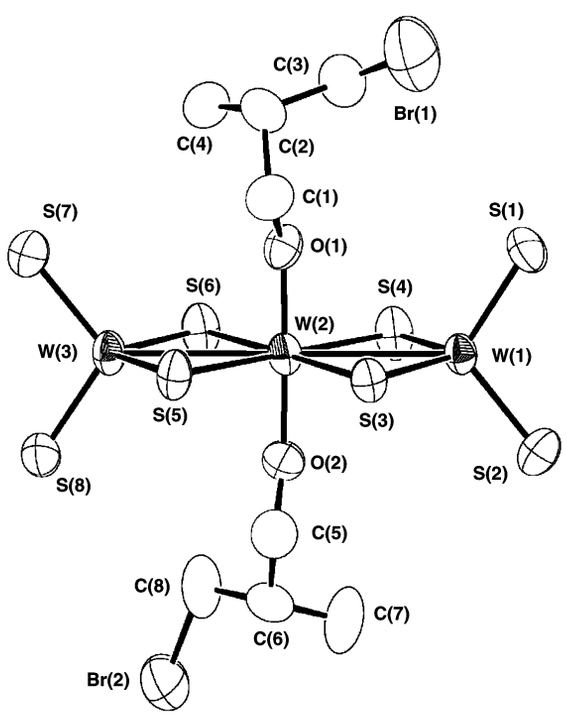

Fig. 3 Structure of $[W_3S_8((S)\text{-}(+)\text{-}OCH_2CH(Me)CH_2Br)_2]^{2-}$ (**7**). The thermal ellipsoids represent 50% probability surfaces. Hydrogen atoms are omitted for clarity.

the complex dianion of **7**, and Table 2 gives its selected bond lengths and angles. The complex dianion consists of a $[W_3S_8]$ core in which the central W(2) atom nearly sits in the least-squares plane defined by S(3)–S(6), and the out-of-plane displacement of W(2) is 0.012 Å. Two chiral (S)-(+)-$OCH_2CH(Me)CH_2Br$ ligands coordinate to W(2) from the top and bottom of the plane, completing an octahedral geometry, where the O(1)–W(2)–O(2) angle is 172.7(5)°. The W(1)–O(1) and W(2)–O(2) bond lengths of 1.886(9) and 1.828(8) Å are comparable to the W–OR distances in $\{HB(Me_2pz)_3\}WOS\{(-)\text{-mentholate}\}$ (1.86(1) Å) and $\{HB(Me_2pz)_3WS_2(OPh)\}$ (1.889(8) Å).[19] The two terminal tungsten atoms, W(1) and W(3), assume a tetrahedral coordination geometry. The W(1)–W(2)–W(3) spine is linear (179.20(3)°), and the mean W–W distance is 2.999 Å. The W–S bond distances can be classified into the following three groups; (1) those around the central W(2) atom (av. 2.453 Å), (2) those between the terminal W atoms and the bridging S atoms (av. 2.256 Å), and (3) the W=S bonds (av. 2.158 Å).

These bond distances of **7** described above are similar to the corresponding values of $[W_3S_9]^{2-}$ [14] and $[W_3OS_8(H_2O)]^{2-}$, while those of $[W_3S_8]^{2-}$ are significantly shorter except for the W=S distances,[16] as summarized in Table 3. In $[W_3S_8((S)\text{-}(+)\text{-}OCH_2CH(Me)CH_2Br)_2]^{2-}$ (**7**), $[W_3S_9]^{2-}$, and $[W_3OS_8(H_2O)]^{2-}$, the formal oxidation states of the three W atoms may be assigned as +6, +4, and +6. The longer W(central)–S distances, relative to the W(terminal)–S bonds, support this view, although the higher coordination number of W(central) could be another reason for the elongation. On the other hand, the formal oxidation states of the W atoms of $[W_3S_8]^{2-}$ can be considered as +6, +2, +6, and the central W atom adopts a square-planar coordination geometry with a slight distortion toward a tetrahedral structure. It is also interesting to compare the structure of **7** with that of $[Fe(WS_4)_2(DMF)_2]^{2-}$.[21] This linear W–Fe–W cluster is similar to **7** in that the central Fe(II) is coordinated by four sulfur atoms of the $[WS_4]^{2-}$ units and it is further coordinated by two DMF molecules with a *trans* configuration.

Spectroscopic properties

Complexes **1**–**7** were characterized by ^{1}H NMR, IR, and UV-vis spectra, and THF solutions of **1**–**6** were subject to ESI mass spectral analysis. All the ^{1}H NMR spectra measured in $CDCl_3$ gave signal intensities consistent with the proposed formulation. No sign of association of the alkylated complexes in solution was detected either in the ^{1}H NMR spectra or the ESI mass spectra. The observed IR and UV-vis bands are summarized in Table 4. The IR spectra of **1**–**4** feature bands in the 488–493 and 413–461 cm^{-1} regions, which are assigned to the W=S and W–SR stretching vibrations, respectively. The Mo=S and Mo–SR stretching bands of **5** and **6** appear in the regions of 508–511 and 433–482 cm^{-1}, and they are all shifted to higher wave numbers compared with the corresponding IR bands of the W complexes, **1**–**4**. The IR spectrum of **7** also shows the W=S band at 487 cm^{-1} and the W–S_{br} band at 455 cm^{-1}. The electronic spectra of **2**–**6** in CH_3CN display four absorption peaks in the region of 282–595 nm, while the spectrum of **1** shows only three. Since the metal atoms of **2**–**6** have d^0 electronic configurations, these absorptions must arise from the S-to-W(Mo) charge transfer transitions. The four absorptions

Table 3 Comparison of selected bond lengths (Å) of linear trinuclear polythiotungstate anions

	Formal oxidation states	Mean W–W	Mean W_{cent}–S_{br}	Mean W_t=S_t	Mean W_t–S_{br}	W_{cent}–S (O)	Ref.
$[W_3S_9]^{2-}$	+6, +4, +6	2.965	2.403	2.142	2.254	2.070 (W_{cent}=S_t)	14
$[W_3OS_8(H_2O)]^{2-}$	+6, +4, +6	2.962	2.432	2.163	2.261	1.67 (W_{cent}=O), 2.46 (W_{cent}–OH_2)	15
$[W_3S_8]^{2-}$	+6, +2, +6	2.871	2.344	2.152	2.237		16
$[W_3S_8((S)$-(+)-$OCH_2CH(Me)CH_2Br)_2]^{2-}$	+6, +4, +6	2.999	2.453	2.158	2.256	1.886, 1.828(6) (W_{cent}–O)	This work

Table 4 IR and UV-vis spectral data for **1**–**7**

	IR (KBr): ν(M–S)/cm^{-1}	UV-vis (CH_3CN): λ_{max}/nm (ε/M^{-1} cm^{-1})
$[PPh_4][(n\text{-hexyl-S})WS_3]$ (**1**)	490 (s), 455 (w), 413 (w)	281 (12000), 382 (7200), 437 (840)
$[PPh_4][(ClCH_2CH_2CH_2CH_2\text{–S})WS_3]$ (**2**)	492 (s), 450 (w)	285 (16000), 382 (9700), 436 (1700), 505 (250)
$[PPh_4][(mthp\text{-S})WS_3]$ (**3**)	488 (s), 453 (m)	282 (15000), 382 (7900), 437 (1500), 512 (330)
$[PPh_4][(edo\text{-S})WS_3]$ (**4**)	493 (s), 461 (w), 419 (w)	285 (8000), 382 (4900), 435 (1000), 510 (230)
$[PPh_4][(mthp\text{-S})MoS_3]$ (**5**)	508 (s), 482 (m), 441 (w)	317 (7600), 450 (4600), 514 (1300), 593 (600)
$[PPh_4][(edo\text{-S})MoS_3]$ (**6**)	511 (s), 482 (m), 433 (w)	317 (6300), 450 (3800), 511 (950), 595 (300)
$[PPh_4]_2[W_3S_8((S)$-(+)-$CH_2CH(Me)CH_2Br)_2]$ (**7**)	487 (s) 455 (m)	308 (13800), 398 (22400), 450 (3500)

of the W complex **3** at 282, 382, 437, and 512 nm are all red shifted to 317, 450, 514, and 593 nm for the Mo congener **5**. The bathochromic shifts amount to 0.49, 0.49, 0.43, and 0.33 eV, respectively, and the shifts are probably due to the lower positioning of vacant 4d orbital levels of Mo relative to the vacant 5d levels of W. Similar bathochromic shifts were observed in going from **4**(W) to **6**(Mo). In the electronic spectrum of **7**, there are three peaks in the 300–450 nm region.

The negative ESI mass spectra of **1**–**6** in dry THF clearly showed the signals arising from the parent $[(RS)MS_3]^-$ anions. As an example, we compare in Fig. 4 the observed signals (top) and the theoretical isotopic distribution (below) for $[(mthp\text{-S})MoS_3]^-$ (**5**). In addition to the parent anion signals described above, each ESI mass spectrum contains an isotopic cluster assignable to $[MS_3(SH)]^-$, appearing at m/z = 313.0 for M = W or m/z = 226.8 for M = Mo. The mechanism of the formation of $[MS_3(SH)]^-$ is not very clear, but we presume that the mercapto complexes were generated from $[(RS)MS_3]^-$ during the measurement. Formation of the $[WS_3(SH)]^-$ anion was reported upon protonation of $[WS_4]^{2-}$ in a dilute acidic media,[22] while the molybdenum analog has not been isolated yet. Table 5 lists the peaks observed for **1**–**6** along with their relative intensities, where only the highest peak in each isotopic cluster is given. The relative intensities of the signals for $[(RS)MS_3]^-$ and $[MS_3(SH)]^-$ vary substantially. If the intensity ratio of $[(RS)MS_3]^-/[MS_3(SH)]^-$ is a measure of stability of $[(RS)MS_3]^-$ under the experimental conditions, the relative stability would be in the order of **5** > **6** > **3** > **4** > **1** > **2**. Thus complexes containing mthp and edo ligands (**3**–**6**) may exhibit higher stability than **1** and **2**.

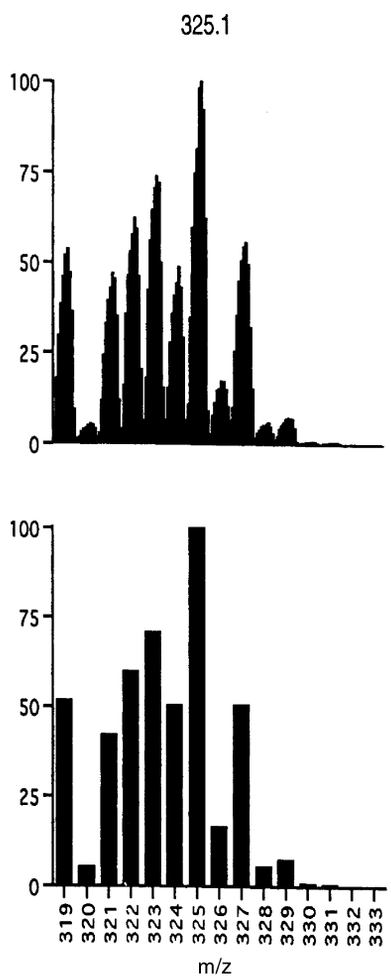

Fig. 4 The observed negative-ion ESI mass spectrum (top) and the calculated isotope pattern (below) of $[(mthp\text{-S})MoS_3]^-$ (**5**).

Conclusion

Alkylation reactions of $[PPh_4]_2[MS_4]$ (M = W, Mo) with various substituted haloalkanes have been investigated. We were successful in isolating a series of the alkylated complexes, $[PPh_4][(RS)MS_3]$, although they are not very stable in solution because facile degradation occurs to give polythiotungstates. On the other hand, the reaction between $[PPh_4]_2[WS_4]$ and (*S*)-(+)-3-bromo-2-methyl-1-propanol gave rise to a trinuclear complex $[PPh_4]_2[W_3S_8((S)$-(+)-$OCH_2CH(Me)CH_2Br)_2]$. The OH group of (*S*)-(+)-3-bromo-2-methyl-1-propanol seems to be acidic due to the bromo substituent, and it is more reactive toward $[WS_4]^{2-}$ than the bromide itself. The reported complexes, except for $[PPh_4][(n\text{-hexyl-S})MS_3]$, were structurally characterized by X-ray analysis, and their electronic properties and solution behavior were examined by IR, UV-vis, and ESI-mass spectroscopy. The newly synthesized complexes of the type $[PPh_4][(RS)MS_3]$ will be useful as convenient precursors for the construction of various homo- and hetero-metallic sulfido clusters.

Experimental

General procedures

All manipulations were carried out under argon using standard Schlenk-line techniques. $(NH_4)_2[MS_4]$ (M = Mo, W) and other chemicals were purchased from commercial sources and were used as received. $[PPh_4]_2[MS_4]$ (M = W, Mo) was prepared by

Table 5 Electrospray ionization mass spectral data for **1**–**6**[a]

	Compound	Peak (*m*/*z*)	Relative intensity (%)
1	$[(n\text{-hexyl-S})WS_3]^-$	397.1	100
	$[WS_3(SH)]^-$	313.0	59
2	$[(ClCH_2CH_2CH_2CH_2CH_2S)WS_3]^-$	405.1	39
	$[WS_3(SH)]^-$	313.0	100
3	$[(mthp\text{-}S)WS_3]^-$	411.1	100
	$[WS_3(SH)]^-$	313.0	18
4	$[(edo\text{-}S)WS_3]^-$	427.1	100
	$[WS_3(SH)]^-$	313.0	23
5	$[(mthp\text{-}S)MoS_3]^-$	325.1	100
	$[MoS_3(SH)]^-$	226.8	8
6	$[(edo\text{-}S)MoS_3]^-$	341.0	100
	$[MoS_3(SH)]^-$	226.8	13

[a] Only the highest peak in each isotope cluster is presented.

addition of $(NH_4)_2[MS_4]$ in water solution to an aqueous solution of PPh_4Br. The resulting solid was collected by filtration, washed with H_2O, EtOH and Et_2O and dried *in vacuo*. All solvents except for water were predried over activated molecular sieves and refluxed over the appropriate drying agents under argon. Elemental analyses for C, H, N, and S were performed on a LECO-CHNS-932 elemental analyzer. ^{1}H NMR spectra were recorded on a Varian UNITYplus-500 spectrometer at ambient temperature unless otherwise noted. ^{1}H NMR chemical shifts are reported in ppm relative to undeuterated chloroform contained in $CDCl_3$. FT-IR spectra in the range 4000–400 cm^{-1} were recorded as KBr pellets on a Perkin-Elmer 2000 FT-IR spectophotometer. UV-vis spectra were measured using a JASCO V560 spectrophotometer. Electrospray ionization (ESI) mass spectra were recorded on an API 300 Triple Quadruple LC/MS/MS mass spectrometer (Perkin-Elmer Sciex Instruments). Samples were introduced to the spectrometer as a THF solution (*ca.* 0.1 M) at a flow rate of 3 μL min^{-1} using a syringe pump (Harvard Apparatus). The potential of the electrospray probe capillary was maintained at 3.5 kV and the orifice-to-skimmer potential (cone voltage) at 20 V.

Preparations

$[PPh_4][(n\text{-}C_6H_{13}S)WS_3]$ (1). $[PPh_4]_2[WS_4]$ (0.50 g, 0.50 mmol) was dissolved in CH_3CN (50 mL), to which n-hexylbromide (0.42 mL, 3 mmol) was added. The solution was stirred for 2 h at room temperature and the color changed to red. The solvent was removed *in vacuo*, and the residue was treated with THF (40 mL) and filtered. After the THF solution was concentrated to *ca.* 4 mL, Et_2O (8 mL) was layered onto the filtrate to form red prisms of **1** in 4 days, which were isolated by filtration, washed with THF–Et_2O (1 : 4), and dried *in vacuo*. Yield: 0.25 g (73%). Anal. calc. for $C_{30}H_{33}PS_4W$: C, 48.91; H, 4.52; S 17.41. Found: C, 49.16; H, 4.60; S, 17.81%. ^{1}H NMR ($CDCl_3$, 500 MHz): δ 7.64–7.91 (m, 20H, PPh_4), 3.27 (t, 2H, SCH_2), 1.69 (m, 2H, SCH_2CH_2), 1.33 (m, 2H, $SCH_2CH_2CH_2$), 1.24 (m, 4H, $SCH_2CH_2CH_2CH_2CH_2$), 0.84 (t, 3H, $SCH_2CH_2CH_2CH_2CH_2CH_3$).

$[PPh_4][(ClCH_2CH_2CH_2CH_2S)WS_3]$ (2). 1,4-Dichlorobutane (0.68 mL, 3.0 mmol) was added to a CH_3CN solution (50 mL) of $[PPh_4]_2[WS_4]$ (0.50 g, 0.50 mmol). The solution was stirred for 4 days at room temperature and the color gradually turned red. From a workup similar to the one used for the isolation of **1**, red prisms of **2** were obtained in 63% yield. Anal. calc. for $C_{28}H_{28}ClPS_4W$: C, 45.26; H, 3.81; S, 17.26. Found: C, 44.89; H, 3.75; S, 17.41%. ^{1}H NMR ($CDCl_3$, 500 MHz): δ 7.57–7.86 (m, 20H, PPh_4), 3.57 (t, 2H, $ClCH_2$), 3.48 (t, 2H, SCH_2), 1.93 (m, 4H, $SCH_2CH_2CH_2CH_2Cl$).

$[PPh_4][(mthp\text{-}S)WS_3]$ (3). Bmthp (0.78 mL, 3.0 mmol) was added to a CH_3CN solution (50 mL) of $[PPh_4]_2[WS_4]$ (0.50 g, 0.50 mmol), and the solution was stirred for 48 h at room temperature. The color of the solution slowly changed from yellow to red. From a workup similar to that used for the isolation of **1**, red prisms of **3** were obtained in 81% yield. Anal. calc. for $C_{30}H_{31}OPS_4W$: C, 48.00; H, 4.17; S, 17.08. Found: C, 47.68; H, 4.09; S, 16.77%. ^{1}H NMR ($CDCl_3$, 500 MHz): δ 7.65–7.92 (m, 20H, PPh_4), 3.92 (m, 1H, OCH_{eq}), 3.66 (m, 1H, OCH_2S), 3.47 (m, 1H, OCH_{ax}), 3.37, 3.31 (m, 2H, CH_2S), 1.79 (m, 2H, OCH_2CH_{eq} + $OCHCH_{eq}$), 1.48 (m, 3H, OCH_2CH_{ax} + $OCH_2CH_2CH_{eq}$ + $OCHCH_{ax}$), 1.23 (m, 1H, $OCH_2CH_2CH_{ax}$).

$[PPh_4][(edo\text{-}S)WS_3]$ (4). Bedo (0.46 mL, 3.0 mmol) was added to a CH_3CN solution (50 mL) of $[PPh_4]_2[WS_4]$ (0.50 g, 0.50 mmol). The solution was stirred for 8 h at room temperature and the color gradually turned red. From a workup similar to that used for the isolation of **1**, red prisms of **4** were obtained in 71% yield. Anal. calc. for $C_{30}H_{31}O_2PS_4W$: C, 47.00; H, 4.08; S, 16.73. Found: C, 47.11; H, 4.09; S, 16.04%. ^{1}H NMR ($CDCl_3$, 500 MHz): δ 7.64–7.91 (m, 20H, PPh_4), 4.65 (t, $^3J_{HH}$ = 5.5 Hz, 1H, O_2CH), 4.03 (m, 2H, OCH_{eq}), 3.74 (m, 2H, OCH_{ax}), 3.31 (t, $^3J_{HH}$ = 7.0 Hz, 2H, SCH_2), 1.97–2.06 (m, 3H, SCH_2CH_2 + $CH_{eq}(CH_2O)_2$), 1.29 (m, 1H, $CH_{ax}(CH_2O)_2$).

$[PPh_4][(mthp\text{-}S)MoS_3]$ (5). To a red suspension of $[PPh_4]_2[MoS_4]$ (0.22 g, 0.24 mmol) in 50 mL CH_3CN–THF (2 : 3 v/v) was added bmthp (0.38 mL, 1.48 mmol). The mixture was stirred for 30 h at room temperature, resulting in a homogeneous dark red–brown solution. After removing the solvents *in vacuo* at 0 °C, the residue was extracted with 40 mL THF and filtered. The filtrate was concentrated to *ca.* 4 mL and filtered again. Diethyl ether (8 mL) was layered onto the filtrate and left standing at −5 °C for 5 days, from which dark red–brown prisms of **5** were isolated in 15% yield. Anal. calc. for $C_{30}H_{31}MoOPS_4$: C, 54.37; H, 4.72; S, 19.35. Found: C, 54.24; H, 4.68; S, 19.51%. ^{1}H NMR ($CDCl_3$, 500 MHz): δ 7.63–7.89 (m, 20H, PPh_4), 3.92 (m, 1H, OCH_{eq}), 3.63 (m, 1H, OCH_2S), 3.47 (m, 1H, OCH_{ax}), 3.18, 3.08 (m, 2H, CH_2S), 1.80 (m, 2H, OCH_2CH_{eq} + $OCHCH_{eq}$), 1.48 (m, 3H, OCH_2CH_{ax} + $OCH_2CH_2CH_{eq}$ + $OCHCH_{ax}$), 1.23 (m, 1H, $OCH_2CH_2CH_{ax}$).

$[PPh_4][(edo\text{-}S)MoS_3]$ (6). A mixture of $[PPh_4]_2[MoS_4]$ (0.22 g, 0.24 mmol) and 2-(bromoethyl)-1,3-dioxane (0.22 mL, 1.48 mmol) in 50 mL CH_3CN–THF (2 : 3 v/v) was stirred for 48 h at room temperature to form a dark red–brown solution containing a small amount of unreacted $[PPh_4]_2[MoS_4]$ as a red solid. After a workup similar to that used for the isolation of **5**, dark red–brown prisms of **6** were isolated in 12% yield. Anal. calc. for $C_{30}H_{31}MoO_2PS_4$: C, 53.08; H, 4.61; S, 18.89. Found: C, 53.24; H, 4.68; S, 19.51%. ^{1}H NMR ($CDCl_3$, 500 MHz): δ 7.63–7.90 (m, 20H, PPh_4), 4.65 (t, $^3J_{HH}$ = 5.5 Hz, 1H, O_2CH), 4.04

Table 6 Crystallographic data for **2**–**7**

Compound	**2**	**3**	**4**	**5**	**6**	**7**
Empirical formula	$C_{28}H_{28}ClPS_4W$	$C_{30}H_{31}OPS_4W$	$C_{30}H_{31}O_2PS_4W$	$C_{30}H_{31}OPMoS_4$	$C_{30}H_{31}O_2PS_4Mo$	$C_{56}H_{56}Br_2O_2P_2S_8W_3$
M_r	743.05	750.64	766.64	662.73	678.73	1790.84
Crystal system	Monoclinic	Triclinic	Monoclinic	Triclinic	Monoclinic	Triclinic
Space group	$P2_1/c$ (no. 14)	$P\bar{1}$ (no. 2)	$P2_1/c$ (no. 14)	$P\bar{1}$ (no. 2)	$P2_1/c$ (no. 14)	$P\bar{1}$ (no. 1)
a/Å	9.806(10)	11.156(6)	9.716(1)	11.123(2)	9.7259(6)	12.543(3)
b/Å	13.56(2)	14.438(3)	18.398(8)	14.434(3)	18.4227(8)	13.160(4)
c/Å	22.78(1)	11.046(4)	17.666(6)	11.027(2)	17.6303(8)	9.969(3)
α/°		100.80(2)		100.77(2)		101.70(3)
β/°	97.54(6)	117.66(3)	96.68(2)	117.49(1)	96.682(2)	100.97(3)
γ/°		85.52(3)		85.59(2)		73.06(3)
V/Å^3	3003(4)	1547(1)	3136(1)	1542.7(6)	3137.5(2)	1526.2(8)
Z	4	2	4	2	4	1
D_c/g cm^{-3}	1.643	1.611	1.623	1.427	1.437	1.948
μ(Mo-Kα)/mm^{-1}	4.287	4.079	4.030	0.768	0.760	7.324
Reflections with $I > 3\sigma(I)$	2940	3960	3658	3884	2674	5846
Parameters	334	334	406	334	406	658
R[a]	0.052	0.035	0.038	0.041	0.053	0.030
R_w[b]	0.076	0.038	0.047	0.051	0.062	0.047
GOF(F^2)[c]	3.09	1.38	1.43	1.86	2.18	1.20
Largest residual peak and hole/e Å^{-3}	1.19 and −1.51	1.34 and −0.55	0.74 and −0.57	0.72 and −0.26	0.52 and −0.48	1.94 and −1.62

[a] $R = \Sigma||F_o| - |F_c||/\Sigma F_o|$. [b] $R_w = \{w\Sigma(|F_o| - |F_c|)^2/\Sigma w|F_o|^2\}^{1/2}$. [c] GOF = $\{\Sigma w(|F_o| - |F_c|)^2/(M - N)\}^{1/2}$, where M is the number of reflections and N is the number of parameters.

(m, 2H, OCHH_{eq}), 3.74 (m, 2H, OCHH_{ax}), 3.14 (t, $^3J_{HH}$ = 7.0 Hz, 2H, SCH_2), 1.96–2.06 (m, 3H, SCH$_2$CH_2 + CHH_{eq}-(CH$_2$O)$_2$), 1.29 (m, 1H, CHH_{ax}(CH$_2$O)$_2$).

[PPh$_4$]$_2$[W$_3$S$_8$((*S*)-(+)-OCH$_2$CH(Me)CH$_2$Br)$_2$] (7). A solution of [PPh$_4$]$_2$[WS$_4$] (0.50 g, 0.50 mmol) in CH$_3$CN (50 mL) was treated with optically pure (*S*)-(+)-3-bromo-2-methyl-1-propanol (0.63 mL, 3.0 mmol). As the reaction mixture was stirred at room temperature, the yellow solution became red over a period of 2 h. With a workup similar to that used for **1**, leaf-like dark red crystals of **7** and dark red microcrystalline solids of [PPh$_4$]$_2$[W$_3$S$_9$] were formed in 3 days. These two complexes were separated manually. Yield: 0.095 g, 32% for **7**, 0.12 g, 47% for [PPh$_4$]$_2$[W$_3$S$_9$]. Anal. calc. for $C_{56}H_{56}Br_2O_2P_2S_8W_3$: C, 37.56; H, 3.16; S, 14.32. Found: C, 37.51; H, 3.15; S, 14.22%. ^{1}H NMR (DMSO-d$_6$, 500 MHz): δ 7.72–7.98 (40H, m, PPh$_4$), 3.60 (d, 4H, CH_2O), 3.33 (d, 4H, CH_2Br), 1.97 (m, 2H, CH), 1.10 (d, 6H, CH_3). [PPh$_4$]$_2$[W$_3$S$_9$] was identified by IR, UV-vis, ^{1}H NMR spectra, and elemental analysis.

X-Ray crystallography

Diffraction data for **2**–**5** and **7** were collected at ambient temperatures on a Rigaku AFC7R diffractometer, and those for **6** were measured at −100 °C under a cold nitrogen stream on a Rigaku RASA-7 Quantum system equipped with an ADSC CCD detector and an MSC d*TREK software package. These diffractometers use graphite-monochromated Mo-Kα radiation (0.71069 Å). Single crystals of **2**–**5** and **7** grown from THF–Et$_2$O and sealed in glass capillaries under argon. Cell constants and an orientation matrix for data collection were determined by least-squares methods from the setting angles of 25 carefully centered reflections (24 reflections in the case of **5**). Three representative reflections were monitored at regular intervals, which showed no sign of significant decay throughout the data collection except for **2**. In the case of **2**, intensities of the standard reflections decreased by 17.6% over the period of data collection. An empirical absorption correction was applied by the ψ-scan technique, which resulted in transmission factors ranging from 0.55 to 1.00 for **2**, 0.75 to 1.00 for **3**, 0.70 to 1.00 for **4**, 0.85 to 1.00 for **5**, and 0.69 to 1.00 for **7**. A small crystal of **6**, 0.15 × 0.1 × 0.1 mm, was mounted at the top of a thin quartz fiber using viscous oil, which was set immediately on a goniometer head under a cold nitrogen stream. Four data frames were recorded at 0.5° increments of ω, and the preliminary unit cell parameters were determined therefrom. The data collection was made with 0.5° intervals of ω for a duration of 97 s, and a total of 462 frames were obtained. The frame data were integrated using a d*TREK program package, and the data set was corrected for absorption using a REQAB program. The reflection data of **2**–**7** were corrected for Lorentz and polarization effects.

The structures of **3** and **5** were solved by direct methods[23] while those of **2**, **4**, **6**, and **7** were solved by the heavy-atom Patterson method,[24] and they were expanded using Fourier techniques.[25] In the case of **2**, C(4) and Cl(1) were found to be disordered over two positions, which were refined with occupancy factors of 0.5/0.5. For **4** and **6**, carbon [except for C(3)] and oxygen atoms of the edo moiety to S(1) were also disordered over two orientations with 0.5/0.5 occupancy. All non-hydrogen atoms were refined anisotropically. Hydrogen atoms except for those at disordered atoms in **2**, **4** and **6** were placed at the calculated positions without refinement. Neutral atom scattering factors were taken from Cromer and Waber,[26a] and anomalous dispersion effects were included in F_c.[26b] Crystallographic calculations were carried out with a teXsan crystallographic software package of the Molecular Structure Corporation (1985 and 1992). Crystallographic data for **2**–**7** are summarized in Table 6.

CCDC reference numbers 168948–168953.

See http://www.rsc.org/suppdata/dt/b1/b106572f/ for crystallographic data in CIF or other electronic format.

Acknowledgements

Jian-Ping Lang thanks the Japan Society for the Promotion of Science (JSPS) for a postdoctoral fellowship at Nagoya University.

References

1 A. Müller, E. Diemann, R. Jostes and H. Bögge, *Angew. Chem., Int. Ed. Engl.*, 1981, **20**, 934.
2 R. H. Holm, *Pure Appl. Chem.*, 1995, **67**, 2117.
3 *Molybdenum Enzymes, Cofactors and Model Systems (ACS Symposium Series 535)*, eds. E. I. Stiefel, D. Coucouvanis and W. E. Newton, American Chemical Society, Washington, DC, 1993.

4 D. Coucouvanis, *Acc. Chem. Res.*, 1991, **24**, 1.
5 M. D. Curtis, *Appl. Organomet. Chem.*, 1992, **6**, 429.
6 T. B. Rauchfuss, in *Progress in Inorganic Chemistry*, ed. S. J. Lippard, Wiley-Interscience, New York, 1991, vol. 39, p. 259.
7 (*a*) M. Rakowski DuBois, *Chem. Rev.*, 1989, **89**, 1; (*b*) T. R. Halbert, C. T. Ho, E. I. Stiefel, R. R. Chianelli and M. Daage, *J. Catal.*, 1991, **130**, 116; (*c*) B. C. Gates, *Catalytic Chemistry*, Wiley-Interscience, New York, 1991.
8 (*a*) S. Shi, W. Ji, S.-H. Tang, J.-P. Lang and X.-Q. Xin, *J. Am. Chem. Soc.*, 1994, **116**, 3615; (*b*) J.-P. Lang, K. Tatsumi, J.-M. Lu, P. Ge, W. Ji and S. Shi, *Inorg. Chem.*, 1996, **35**, 7924.
9 (*a*) E. Ruizhitzky, R. Jimenez, B. Casal, V. Manriquez, A. S. Ana and G. Gonzalez, *Adv. Mater.*, 1993, **5**, 738; (*b*) C. M. Zelenski and P. K. Dorhout, *J. Am. Chem. Soc.*, 1998, **120**, 734.
10 (*a*) P. M. Boorman, M.-P. Wang and M. Parrez, *J. Chem. Soc., Chem. Commun.*, 1995, 999; (*b*) N. L. Kruhlak, M. Wang, P. M. Boorman, M. Parvez and R. McDonald, *Inorg. Chem.*, 2001, **40**, 3141; (*c*) P. M. Boorman, X.-L. Gao, H. B. Kraatz, V. Mozol and M.-P. Wang, in *Tranistion Metal Sulfur Chemistry (ACS Symposium Series 653)*, eds. E. I. Stiefel and K. Matsumoto, American Chemical Society, Washington, DC, 1996, p. 179; (*d*) N. L. Kruhlak, PhD Thesis, University of Calgary, 2001.
11 D. Coucouvanis, S.-J. Chen, B. S. Mandimutrira and C. G. Kim, *Inorg. Chem.*, 1994, **33**, 4429.
12 (*a*) H. Kawaguchi and K. Tatsumi, *J. Am. Chem. Soc.*, 1995, **117**, 3885; (*b*) H. Kawaguchi, K. Yamada, J.-P. Lang and K. Tatsumi, *J. Am. Chem. Soc.*, 1997, **119**, 10343.
13 (*a*) J.-P. Lang, H. Kawaguchi, S. Ohnishi and K. Tatsumi, *Chem. Commun.*, 1997, 405; (*b*) J.-P. Lang, H. Kawaguchi and K. Tatsumi, *Inorg. Chem.*, 1997, **36**, 6447; (*c*) J.-P. Lang and K. Tatsumi, *Inorg. Chem.*, 1998, **37**, 160; (*d*) J.-P. Lang, H. Kawaguchi, S. Ohnishi and K. Tatsumi, *Inorg. Chim. Acta*, 1998, **283**, 136; (*e*) J.-P. Lang, H. Kawaguchi and K. Tatsumi, *J. Organomet. Chem.*, 1998, **509**, 109.
14 A. Müller, H. Bögge, E. Krickmeyer, G. Henkel and B. Krebs, *Z. Naturforsch., Teil B*, 1982, **37**, 1014.
15 (*a*) P. Dhar and S. Chandrasekaran, *J. Org. Chem.*, 1989, **54**, 2998; (*b*) P. Dhar, R. Ranjan and S. Chandrasekaran, *J. Org. Chem.*, 1990, **55**, 3728.
16 A. Müller, R. G. Bhattacharyya, E. Koniger-Ahlborn, R. C. Sharma, W. Ritter, A. Neumann, G. Henkel and B. Krebs, *Inorg. Chim. Acta*, 1979, **37**, L493.
17 S. Bhaduri and J. A. Ibers, *Inorg. Chem.*, 1986, **25**, 3.
18 W. H. Pan, M. E. Leonowicz and E. I. Stiefel, *Inorg. Chem.*, 1983, **22**, 672.
19 F. Sécheresse, J. Lefebvre, J. C. Daran and Y. Jeannin, *Inorg. Chem.*, 1982, **21**, 1311.
20 A. A. Eagle, S. M. Harben, E. R. T. Tiekink and C. G. Young, *J. Am. Chem. Soc.*, 1994, **116**, 9747.
21 P. Stremple, N. C. Baenziger and D. Coucouvanis, *J. Am. Chem. Soc.*, 1981, **103**, 4601.
22 E. Koniger-Ahlborn, H. Schulze and A. Müller, *Z. Anorg. Allg. Chem.*, 1979, **428**, 5.
23 (*a*) P. T. Beurskens, G. Admiraal, G. Beurskens, W. P. Bosman, S. Garcia-Granda, R. O. Gould, J. M. M. Smits and C. Smykalla, ORIENT: The DIRDIF Program System, Technical Report of the Crystallography Laboratory, University of Nijmegen, The Netherlands, 1992; (*b*) SIR92: A. Altomare, M. C. Burla, M. Camalli, M. Cascarano, C. Giacovazzo, A. Guagliardi and G. Polidori, *J. Appl. Crystallogr.*, 1994, **27**, 435; (*c*) H.-F. Fan, SAPI91: Structure Analysis Programs with Intelligent Control, Rigaku Corporation, Tokyo, Japan, 1991.
24 P. T. Beurskens, G. Admiraal, G. Beurskens, W. P. Bosman, S. Garcia-Granda, R. O. Gould, J. M. M. Smits and C. Smykalla, PATTY: The DIRDIF Program System, Technical Report of the Crystallography Laboratory, University of Nijmegen, The Netherlands, 1992.
25 (*a*) P. T. Beurskens, G. Admiraal, G. Beurskens, W. P. Bosman, S. Garcia-Granda, R. O. Gould, J. M. M. Smits and C. Smykalla, DIRDIF92: The DIRDIF Program System, Technical Report of the Crystallography Laboratory, University of Nijmegen, The Netherlands, 1992; (*b*) P. T. Beurskens, G. Admiraal, G. Beurskens, W. P. Bosman, R. de Gelder, R. Israel and J. M. M. Smits, DIRDIF94: The DIRDIF-94 Program System, Technical Report of the Crystallography Laboratory, University of Nijmegen, The Netherlands, 1994.
26 (*a*) D. T. Cromer and J. T. Waber, *International Tables for X-Ray Crystallography*, Kynoch Press, Birmingham, UK, 1974, vol. IV, Table 2.2A; (*b*) J. A. Ibers and W. C. Hamilton, *Acta Crystallogr.*, 1964, **17**, 781.